This is a repository copy of *Ease of matching a load line impedance in a 25 W contiguous mode class BJF−1 broadband amplifier*.

White Rose Research Online URL for this paper:
https://eprints.whiterose.ac.uk/209170/

Version: Accepted Version

Article:
Poluri, N. orcid.org/0000-0002-3664-8322 and De Souza, M.M. orcid.org/0000-0002-7804-7154 (2023) Ease of matching a load line impedance in a 25 W contiguous mode class BJF−1 broadband amplifier. IEEE Microwave and Wireless Technology Letters, 33 (2). pp. 181-184. ISSN 2771-957X

https://doi.org/10.1109/lmwc.2022.3209573

© 2022 IEEE. Personal use of this material is permitted. Permission from IEEE must be obtained for all other users, including reprinting/ republishing this material for advertising or promotional purposes, creating new collective works for resale or redistribution to servers or lists, or reuse of any copyrighted components of this work in other works. Reproduced in accordance with the publisher's self-archiving policy.

Reuse
Items deposited in White Rose Research Online are protected by copyright, with all rights reserved unless indicated otherwise. They may be downloaded and/or printed for private study, or other acts as permitted by national copyright laws. The publisher or other rights holders may allow further reproduction and re-use of the full text version. This is indicated by the licence information on the White Rose Research Online record for the item.

Takedown
If you consider content in White Rose Research Online to be in breach of UK law, please notify us by emailing eprints@whiterose.ac.uk including the URL of the record and the reason for the withdrawal request.

eprints@whiterose.ac.uk
https://eprints.whiterose.ac.uk/

Ease of matching a load line impedance in a 25W Contiguous Mode Class BJF^{-1} Broadband Amplifier

Nagaditya Poluri, *Member, IEEE* and Maria Merlyne De Souza, *Sr. Member, IEEE*

***Abstract*— We investigate contiguous modes called "the series of continuum modes" (SCM) and Class BJF^{-1} that offer a resistive component of the load line impedance that is 1.17 times and 1.7 times that of class B respectively. Both these modes result in a similar performance of efficiency, output power and gain, but class BJF^{-1} has a wider design space and is easier to match. An increase in the resistive component of the fundamental impedance of class BJF-1 increases efficiency with minimal impact on the bandwidth for an inductive load. An amplifier designed in class BJF^{-1} using the CGH40025F demonstrates an average efficiency of 70.8 % and output power greater than 28W over a bandwidth from 2.2-3.3 GHz, resulting in a comparable frequency weighted efficiency of 91% when compared with other reported amplifiers with similar fractional bandwidth and output power whilst operating at highest reported frequency (3.3 GHz) using this device.**

***Index Terms*—Power Amplifiers, SRFT, broadband**

I. Introduction

In a mobile communication network, the PA alone consumes 22%, of the share of the transmitter power [1] and is,, a critical component to address the energy demands of 5G technology. Harmonic tuning is an attractive way to address this challenge. Typically, high-efficiency class F/F^{-1} amplifiers can only be achieved over a narrow bandwidth, due to the requirements of their resonator-like harmonic terminations. To address high-frequency dispersion of the matching network over the entire frequency band is more difficult with conventional matching networks and typically involves a trade-off between Pout, efficiency, and bandwidth. Designing a matching network for higher output powers in a single-stage amplifier is even more challenging because of a lower optimal load line resistance and a larger parasitic output capacitance, which must be canceled out by the matching network. To transform low impedance matching networks to 50 ohms with low loss requires special attention as wider transmission lines increase losses and require more sections for matching.

A load matching network topology with distributed inductive components, to account for dispersion of the second harmonic, was proposed in [2]. Their proposed expressions enabled individual control of the second harmonic for each frequency over the bandwidth. Multistage Chebyshev low-pass filters in L-sections were designed to address instability and compensate for the parasitic input and output capacitances of the device [3]. Higher order Chebyshev filters, although more accurate, were shown to result in more complexity, coupling between the transmission line segments, and deviation from simulation [4]. The *a priori* selection of a matching network topology is avoided in the simplified real frequency technique (SRFT) by representing the S-parameters of the network by a rational polynomial [5].

In comparison to continuous modes, the real component of the impedance at the fundamental frequency varies, resulting in a wider range of impedances available in contiguous modes occupying a 2 dimensional on the Smith chart. However, the Bode-Fano limit [6] reveals that an increase of the real component should decrease the bandwidth, for a fixed output capacitance. This work investigates the impact of an increasing resistive component of the impedances in the SCM (series of continuum modes that refer to impedances between class B/J/J* and continuous class F) [7] and class BJF^{-1} (corresponding to impedances between class B/J/J* and continuous class F^{-1}) [8] on the efficiency and bandwidth. Based on this analysis, we design a 2.2 GHz - 3.3 GHz 25 W amplifier using CGH40025. To our knowledge, this is the highest operating frequency using CGH40025 and the first demonstration of contiguous mode techniques for a power level above 16 W.

II. Choosing Amplifier Class and Matching Network

A bias of 28 V drain voltage (V_{dsq}) and a drain current (I_{dsq}) of 300 mA are chosen in this work, as the best compromise between linearity and efficiency. The optimal load line impedance is obtained as 13 Ω which is 2.5 to 3 times lower when compared to the CGH40010F. In this respect, contiguous modes such as SCM and BJF^{-1} are better suited than conventional classes, because the real part of the fundamental impedance can be varied up to 1.7 times [7] and 1.17 times [8] of class B respectively. This aspect will become increasingly important as the industry strives towards 25W MMICs for 5G applications in the Ka-band.

A. Investigation of design space of SCM and class BJF^{-1}

First, we compare the contours of peak efficiency of the SCM and class BJF^{-1} from the simulation of the CGH40025 over the respective design space at 2.6 GHz in Fig. 1. The

Manuscript received on June 30, 2018. Revised on November 5, 2018. Revised on December 11, 2018. The authors are with the EEE department, University of Sheffield, Sheffield, S37HQ, UK (e-mail: n.poluri@sheffield.ac.uk and m.desouza@sheffield.ac.uk). MMS acknowledges support from ENIAC- JU project PARSIMO under grant contract – 270687.

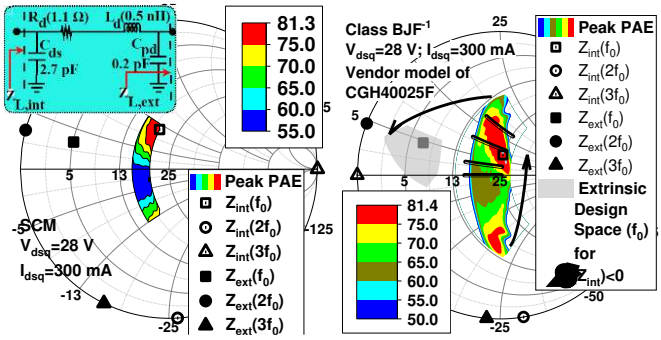

Fig. 1. PAE contours from the CW simulation of the vendor model of CGH40025 over the design space of (a) SCM (b) Class BJF^{-1}.

theoretical impedances at the intrinsic plane are calculated from their formulations and embedded to the extrinsic plane using an approximate parasitic model of the device, shown in the inset of Fig. 1. The source impedance is fixed to 2-5i for both cases. It is seen from the contours that both classes yield similar peak efficiency of 81-83%. Nevertheless, the BJF^{-1} design space is much wider compared to SCM, revealing its advantage. The variation of the efficiency along the constant resistance circle is due to dependence of the harmonics generated from the non-linear drain and feedback capacitances on the load impedance[9]–[11].

Fig. 1 shows that inductive loads at the fundamental frequency ie., impedances with the imaginary component $\Im(Z_{int}(f_0)) > 0$ in class BJF^{-1} present a larger set of impedances which achieve efficiency >75 % when compared to capacitive loads with $\Im(Z_{int}(f_0)) < 0$ in Class BJF^{-1} and SCM. Hence, we focus on the region corresponding to $\Im(Z_{int}(f_0)) > 0$ in class BJF^{-1} for our design and the corresponding design space at the extrinsic plane at 2.6 GHz, is plotted in shaded grey in Fig. 1. We estimate the bandwidth using a matching network, shown in Fig. 2 (a), consisting of an N-section, maximally flat filter, which matches the 50 Ω to $\Re(Z_{L,ext}(f_0))$ and a transmission line (TL) to match $\Re(Z_{L,ext}(f_0))$ to $Z_{L,ext}(f_0)$. The fractional bandwidth (FBW), in this case, is limited either due to the TL line (FBW1) or the filter (FBW2 [6]) and is expressed as $min(FBW1, FBW2)$, where

$$FBW1 = \Re(Z_{L,ext}(f_0))/\Im(Z_{L,ext}(f_0))$$

$$FBW2 = 2 - (4/\pi)\cos^{-1}\left(0.5\sqrt[N]{\Gamma_m/|A|}\right)$$

Where $A=2^{-N}\left|\Re(Z_{L,ext}(f_0)) - Z_0\right|/\left|\Re(Z_{L,ext}) + Z_0\right|$ and the mismatch $(\Gamma_m = \max\left(\left|Z_{L,ext}(f_0) - Z_{MN}(f)\right|\right))$ is the maximum difference between the target impedance $(Z_{L,ext}(f_0))$ and the impedance of the matching network $(Z_{MN}(f))$ over the bandwidth. The estimated FBW at 2.6 GHz for the Z_{int} varied,

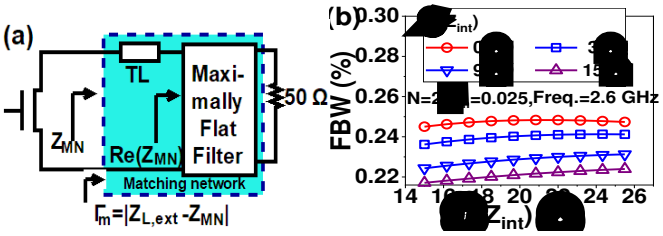

Fig. 2. (a) Equivalent circuit used for analyzing the bandwidth over the design space. (b) Plot of the fractional bandwidth (FBW) as the target fundamental impedance is varied over the design space.

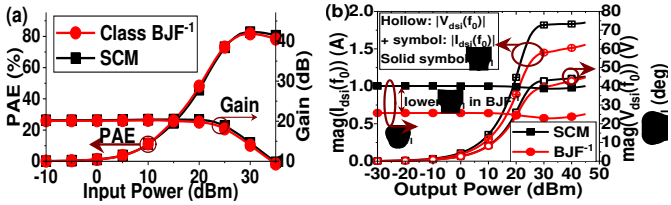

Fig. 3. (a) Simulated Gain, Output power, and PAE for the load impedances of SCM and Class BJF^{-1} choosen from high-efficiency region shown in Fig. 1. (b) The simulated magnitude of fundamental components of intrinsic drain voltage ($V_{dsi}(f_0)$), drain current ($I_{dsi}(f_0)$), and the phase difference between the voltage and current (Ψ_{VI}).

as shown by the dashed lines in Fig. 1, is plotted in Fig. 2 (b), and shows that decreasing the $\Im(Z_{int})$ results in slightly higher bandwidth. The increase in $\Re(Z_{int})$ has a minimal impact on the FBW. However, as can be seen from Fig. 1, an increase in $\Re(Z_{int})$ for $\Im(Z_{int}) > 0$ improves the efficiency indicating that higher efficiency (>75%) can be achieved without sacrificing the FBW. This analysis pertinent only to contiguous mode design represents a best-case scenario because further tuning of the matching network is required to meet the impedances at the second harmonic frequency.

The simulated performance of amplifiers based on SCM and class BJF^{-1} for impedances selected from the high-efficiency regions in Fig. 1, is plotted in Fig. 3 (a). It is seen that the gain, output power, and efficiency are nearly identical for both amplifiers, even though current manipulation (peaking of the current to left or right [14] [8]) in class BJF^{-1} only kicks in at high input powers. Comparing the magnitude of fundamental components of the intrinsic drain voltage ($V_{dsi}(f_0)$), drain current ($I_{dsi}(f_0)$), and the phase difference, in Fig 3 (b), between the voltage and current (Ψ_{VI}) with input power in both classes, it is observed that $|V_{dsi}(f_0)|$ is nearly the same but BJF^{-1} shows a significantly lower Ψ_{VI} compared to SCM. This implies that a reduction in the magnitude of $I_{dsi}(f_0)$ is compensated by a reduction in the phase, leading to their similar amplifier response in Fig. 3 (a). Current manipulated waveforms are particularly beneficial for deep "knee" characteristic semiconductors such as GaN.

B. Choosing matching network

We use the approach which simultaneously optimizes the choice of target impedance with frequency and the matching network topology. The algorithm only requires the class of amplifier, target frequency range, and approximate parasitic network at the drain to be identified [15]. In such a case, the impedances in the design space, matching network expressed as SRFT coefficients, and the performance of the amplifier (PAE in this case) can be expressed as an array[16] which is passed to an optimization algorithm to search for the matching network. A constraint on our matching network is a purely reactive impedance at the second harmonic (ie., 5.2 GHz – 7.8 GHz) to maintain high efficiency. The synthesized load and source matching networks are shown in Fig. 4 and the length and width of the matching network are optimized by EM simulations.

III. Designed Amplifier

A photograph of the designed amplifier is shown in Fig. 5 (a). The measured load matching network is compared with the

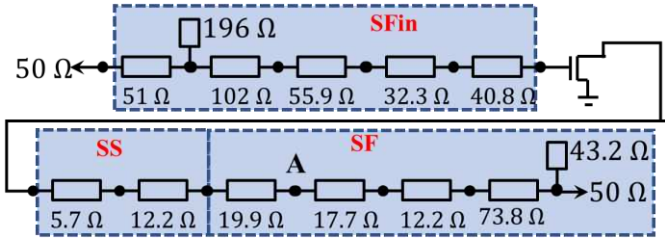

Fig. 4. Synthesized load and source matching network from the SRFT coefficients. Length of all the transmission lines is one-eight of the wavelength at 5 GHz.

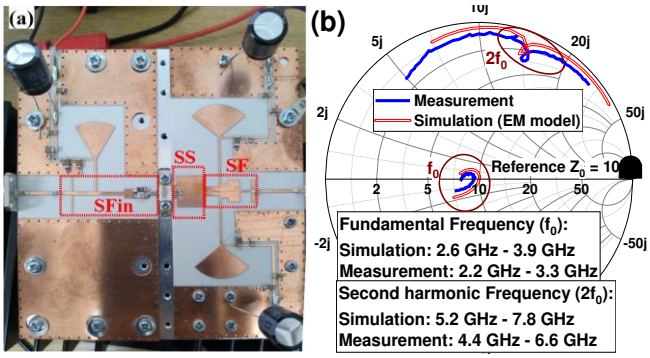

Fig. 5. (a) Photograph of the designed amplifier. (b) Comparison of the measured and simulated load impedances at the fundamental and second harmonic frequencies.

simulation of its EM model in Fig. 5 (b). We observe that the measured impedances are shifted in frequency when compared with simulated impedances both at the fundamental as well as the second harmonic frequencies. This can be resolved in the future by using a taper between the transmission lines to avoid large differences in widths. The amplifier has 400 and 600 MHz shifts at the lower and upper end of the bandwidth consistent with frequency shift in impedances in Fig. 5 (b). Despite this discrepancy, we still achieve an excellent performance which is attributed to the large high-efficiency region, seen in Fig. 1, of the class of amplifier, resulting in immunity to impedance mismatch of class BJF^{-1}. The measured Gain, output power, and Drain efficiency (DE) between 2.2 – 3.3 GHz are plotted in Fig. 6 (a). The amplifier demonstrates an efficiency between 63 -75 % at a saturated output power of 44.5 -45.2 dBm with an average efficiency of 70.8% over the 1.1 GHz (40 %) bandwidth. The gain variation is 2 dB from 11.7-13.9 dB. The frequency weighted efficiency (FE) of the amplifier is 91.6 %(GHz)$^{1/4}$. The reduction of the efficiency at the lower end of the band ie., at 2.2 GHz is because of the resistive component of the second harmonic impedance seen in Fig. 5 (b). The measured IMD3 versus the average output power, with a tone separation of 200 kHz, of the designed amplifier is plotted in Fig. 6 (b). The IMD3 of the amplifier lies below -20 dBc and -25 dBc for power levels up to 40.1 dBm and 42.5 dBm respectively up to 3.2 GHz, except at the edge of the band at 3.3 GHz, demonstrating good linearity. The performance of the measured amplifier is compared with others of a similar FBW and output power in Table 1. The FE of the amplifier is seen to be higher than the reported amplifiers except for [3] and [18]. However, the designed amplifier operates over a higher FBW when compared with [3] and [18]. The plot of FE vs FBW in

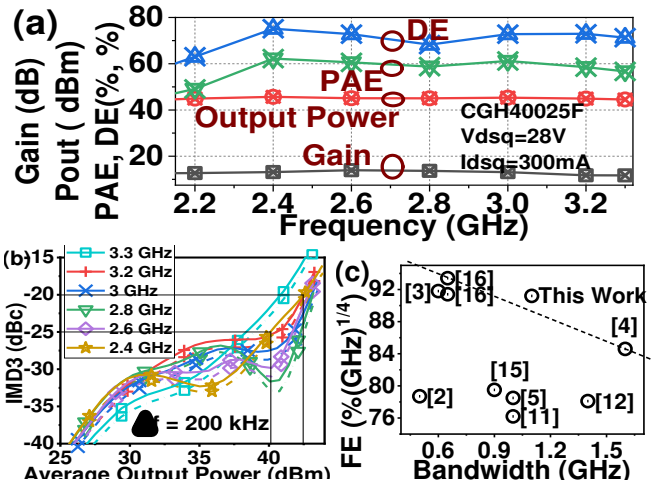

Fig. 6. (a) The measured Drain efficiency (DE), Power-Added Efficiency (PAE), output power, and Gain of designed amplifier with frequency. (b) The measured IMD3 for the two-tone signal with 200 kHz frequency seperation of the designed amplifier. (c) Frequency weighted efficiency (FE) vs bandwidth of the amplifiers reported in literature having similar fractional bandwidth and output power level

Table 1. Comparison of the designed amplifiers with literature have similar fractional bandwidth and output power level

Ref.	BW (GHz, %)	Gain (dB)	Pout (dBm)	DE, AE (%,%)	FE (%$\sqrt[4]{GHz}$)
[12]	1.5-2.5, 50	9.6-12.8	39.5-41.5	60-75, 64.1	76.2
[17]	1.8-2.7, 40	7.6-10	42 - 44.6	48-65.2, 64.9	79.5
[13]	1.5-2.9, 63.6	9.3-13.3	39.4-41.9	60-76.5, 64.1	78.1
[2]	1.8 - 2.3, 25	8.7-13.9	45-47.7	60-76, 66	78.7
[5]	1.9-2.9, 42	10-11.8	44.5-46.6	60-66, 63.1	78.5
[3]	1.7 - 2.3, 30	11.5-13	43.4-45.1	73-80, 77.2	91.8
[4]	1.1-2.7, 84	9.0-12.0	43-44.9	65-75, 72.0	84.6
[18]	2.3-2.95,25	--	43.4-45.3	68-73.8,71.8	91.4
[18]	2.3-2.95,25	--	43.2-44.6	71-74.8,73.4	93.4
This amp.	**2.2-3.3, 40**	**11.7-13.9**	**44.5-45.7**	**63-75, 70.8**	**91.2**

Frequency weighted efficiency(FE)= Average efficiency (AE) multiplied by the fourth root of the centre frequency, as defined in [19]–[21]

Fig 6(c) reveals its superior performance.

IV. Conclusions

A comparison of the series of continuum modes and class BJF^{-1} reveals that both modes result in similar amplifier performance, however, class BJF^{-1} has a larger high-efficiency design space when compared to SCM and offers a higher real part of the impedance than SCM, making it easier to match. This information enables designers in making a judicious choice of engineering waveforms. At 2.6 GHz, inductive loading at the fundamental frequency offers a larger high-efficiency region when compared to capacitive with high efficiency (>75%) without sacrificing the bandwidth by increasing the resistive component, unlike continuous mode amplifiers. Our design methodology achieves an average efficiency of 70.8 % and output power of 28 W over the bandwidth 2.2-3.3 GHz, resulting in one of the highest frequency weighted efficiency when compared with other reported amplifiers with similar fractional bandwidth and output power.

REFERENCE

[1] J. Wu, Y. Zhang, M. Zukerman, and E. K. N. Yung, "Energy-efficient base-stations sleep-mode techniques in green cellular networks: A survey," *IEEE Commun. Surv. Tutorials*, vol. 17, no. 2, pp. 803–826, 2015.

[2] J. Kim, F. Mkadem, and S. Boumaiza, "A high efficiency and multi-band/multi-mode power amplifier using a distributed second harmonic termination," *Eur. Microw. Week 2010, EuMW2010 Connect. World, Conf. Proc. - Eur. Microw. Conf. EuMC 2010*, no. September, pp. 1662–1665, 2010.

[3] M. T. Arnous, P. Saad, S. Preis, and Z. Zihui, "Highly efficient and wideband harmonically tuned GaN-HEMT power amplifier," *2014 20th Int. Conf. Microwaves, Radar Wirel. Commun. MIKON 2014*, pp. 21–24, 2014.

[4] M. T. Arnous, S. E. Barbin, and G. Boeck, "Design of multi-octave highly efficient 20 watt harmonically tuned power amplifier," *2016 21st Int. Conf. Microwave, Radar Wirel. Commun. MIKON 2016*, pp. 16–19, 2016.

[5] D. Y. T. Wu, F. Mkadem, and S. Boumaiza, "Design of a broadband and highly efficient 45w GaN power amplifier via simplified real frequency technique," *IEEE MTT-S Int. Microw. Symp. Dig.*, pp. 1090–1093, 2010.

[6] D. Pozar, *Microwave Engineering*, 4th ed. Wiley, 2005.

[7] J. Chen, S. He, F. You, R. Tong, and R. Peng, "Design of Broadband High-Efficiency Power Amplifiers Based on a Series of Continuous Modes," *IEEE Microw. Wirel. Components Lett.*, vol. 24, no. 9, pp. 631–633, Sep. 2014.

[8] N. Poluri and M. M. De Souza, "High-Efficiency Modes Contiguous With Class B/J and Continuous Class F^{-1} Amplifiers," *IEEE Microw. Wirel. Components Lett.*, vol. 29, no. 2, pp. 137–139, Feb. 2019.

[9] N. Poluri and M. M. De Souza, "Investigation of the Effect of Weak Non-Linearities on P1dB and Efficiency of Class B/J/J* Amplifiers," *IEEE Trans. Circuits Syst. II Express Briefs*, vol. 65, no. 9, pp. 1159–1163, Sep. 2018.

[10] Z. A. Mokhti, J. Lees, C. Cassan, A. Alt, and P. J. Tasker, "The Nonlinear Drain-Source Capacitance Effect on Continuous-Mode Class-B/J Power Amplifiers," *IEEE Trans. Microw. Theory Tech.*, vol. 67, no. 1, pp. 1–7, 2019.

[11] F. Vanaverbeke, P. Saint-Erne, and K. Kim, "Evidence for the Self-Enhanced Class J PA Operating Mode from Harmonic Load-Pull Measurements," *2019 IEEE Top. Conf. RF/Microwave Power Amplifiers Radio Wirel. Appl. PAWR 2019*, pp. 1–4, 2019.

[12] E. Aggrawal, K. Rawat, and P. Roblin, "Investigating continuous class-F power amplifier using nonlinear embedding model," *IEEE Microw. Wirel. Components Lett.*, vol. 27, no. 6, pp. 593–595, 2017.

[13] Y. Mary Asha Latha, K. Rawat, and P. Roblin, "Nonlinear Embedding Model-Based Continuous Class E/F Power Amplifier," *IEEE Microw. Wirel. Components Lett.*, vol. 29, no. 11, pp. 714–717, 2019.

[14] J. H. Kim, S. J. Lee, B. H. Park, S. H. Jang, J. H. Jung, and C. S. Park, "Analysis of High-Efficiency Power Amplifier Using Second Harmonic Manipulation : Inverse Class-F / J Amplifiers," *IEEE Trans. Microw. Theory Tech.*, vol. 59, no. 8, pp. 2024–2036, 2011.

[15] N. Poluri and M. M. De Souza, "Designing a Broadband Amplifier Without Load–Pull," *IEEE Microw. Wirel. Components Lett.*, vol. 31, no. 6, pp. 593–596, Jun. 2021.

[16] N. Poluri and M. M. De Souza, "A methodology to design broadband matching networks for continuum mode PAs," in *Asia-Pacific Microwave Conference Proceedings, APMC*, 2019, vol. 2019-Decem, pp. 1637–1639.

[17] T. Sharma, P. Aflaki, M. Helaoui, and F. M. Ghannouchi, "Broadband gan class-e power amplifier for load modulated delta sigma and 5g transmitter applications," *IEEE Access*, vol. 6, pp. 4709–4719, 2018.

[18] D. R. Barros, L. C. Nunes, P. M. Cabral, and J. C. Pedro, "Impact of the Input Baseband Terminations on the Efficiency of Wideband Power Amplifiers under Concurrent Band Operation," *IEEE Trans. Microw. Theory Tech.*, vol. 67, no. 12, pp. 5127–5138, 2019.

[19] K. Ikossi, "Student High-Efficiency PA Design Competition [TC Contests," *IEEE Microw. Mag.*, vol. 11, no. 1, pp. 112–114, Feb. 2010.

[20] IEEE, "High Efficiency Power Amplifier Student Design Competition," *mtt.org*, 2020. [Online]. Available: https://mtt.org/hepa_student_design_competition/. [Accessed: 27-Jul-2022].

[21] K. Chen and D. Peroulis, "Design of broadband highly efficient harmonic-tuned power amplifier using in-band continuous class-F-1/F mode transferring," *IEEE Trans. Microw. Theory Tech.*, vol. 60, no. 12, pp. 4107–4116, 2012.